Available online at www.sciencedirect.com

ScienceDirect

Procedia CIRP 75 (2018) 45–50

www.elsevier.com/locate/procedia

15th CIRP Conference on Computer Aided Tolerancing – CIRP CAT 2018

Quality-driven Optimization of Assembly Line Configuration for Multi-Station Assembly Systems with Compliant Non-ideal Sheet Metal Parts

Vahid Jandaghi Shahi[a,*], Abolfazl Masoumi[a], Pasquale Franciosa[b], Darek Ceglarek[b]

[a]School of Mechanical Engineering, College of Engineering, University of Tehran, Tehran, 11155- 4563, Iran
[b]Digital Lifecycle Management (DLM), WMG, University of Warwick - CV47AL Coventry, UK

* Corresponding author. Tel.: +98-912-253-3684; *E-mail address:* v_jandaghi@ut.ac.ir

Abstract

Final product quality is affected by both defects generation as well as defects propagation through the multi-station assembly system. Less quantifiable understood is quality defects propagation which depends on assembly line configuration. This paper focuses on modelling and optimization of multi-station assembly line configuration for systems with compliant non-ideal sheet-metal parts. The proposed methodology is based on: (1) assembly sequence generation; (2) multi-station assembly variation propagation model and simulations considering batch of non-ideal parts, station-to-station repositioning error and spring-back phenomenon; (3) development of assembly configuration index; and, (4) calculation of optimal configuration based on stochastic robust optimization. The methodology is demonstrated using automotive front-rail subassembly process.

Peer-review under responsibility of the Scientific Committee of the 15th CIRP Conference on Computer Aided Tolerancing - CIRP CAT 2018.

Keywords: Non-ideal compliant sheet metal-parts; Assembly configuration; Stochastic optimization; Variation response method

1. Introduction

Compliant sheet metal parts in automotive body are assembled in a hierarchical Multi-Station Assembly (MSA) system where dimensional variations are propagated and accumulated at each level of the assembly process. Inherent dimensional variations in MSA are heavily affected by inevitable manufacturing errors, such as part dimensional and geometrical errors (GD&T), fixture and tool deviations, and assembly process factors (number of stations, fixtures layout, and assembly sequence) [1,2]. MSA systems consist of sequential operations where variation at each station affects downstream stations. Moreover, station-to-station interactions introduced by repositioning of parts/sub-assemblies and releasing of fixtures is recognized among the most important factors affecting assembly quality [3].

Many methods have been proposed in the past two decades to model variation-induced quality of compliant assemblies in single- and multi-station assembly processes. They can be categorized into three major groups related to dimensional variation: (i) modeling; (ii) minimization in design; and, (iii) reduction in production.

In the first group, the Method of Influence Coefficients (MIC), which was originally presented by Liu and Hu [4], models the effect of part deviations and spring-back on assembly variation by applying linear mechanics and statistics. The method was applied to single-station assembly. Then, Camelio et al. [3] extended MIC to model MSA systems through state-space model. Chang and Gossard [5] proposed a new variation simulation model based on Place, Clamp, Fasten and Release (PCFR) cycle for single-station assembly process, assuming ideal parts which was then expanded to multi-station system with compliant parts [6]. Stream-of-variation theory applied to parallel and series multi-station assembly systems was introduced in [7–9].

A non-linear FEA approach was developed by Xie et al. [10] to solve the contact problem in assembly of compliant parts. In order to speed-up the assembly process simulation considering part-to-part intersection, Ungemach and Mantwill [11] integrated a linear contact search and a contact equilibrium criterion with MIC. A linear methodology called Statistical Variation Analysis and Finite Element Analysis (SVA–FEA) was introduced by Gerbino et al. [12] and it is based on sensitivity matrix and linear contact assumptions. The method models ideal shape of the parts and localized

2212-8271 © 2018 The Authors. Published by Elsevier B.V.
Peer-review under responsibility of the Scientific Committee of the 15th CIRP Conference on Computer Aided Tolerancing - CIRP CAT 2018.
10.1016/j.procir.2018.02.022

deviations are assumed to be independent [13]. This method was then extended by Franciosa et al. [14,15] to simulate the PCFR cycle considering non-ideal parts with morphing mesh technique. However, this work was limited to single-station assembly systems.

In the second group, many researches have been reporting on dimensional errors reduction for assembly of compliant parts through Assembly Process Planning (APP) which entails two major streams: (1) “fixture configuration” which deals with locator’s scheme and layout optimization in assembly process [16-20]; and, (2) Assembly Sequence Planning (ASP) such as part assembly sequence and line configuration strategy [21-25]. This paper focuses on assembly sequence for multi-station assembly systems, and its impact on final assembly quality. Camelio et al. [16] have used MIC and nonlinear programming method to find the optimal fixture position in single-station assembly. Liao et al. [17] proposed an algorithm to integrate the MIC and mode-pursuing sampling method to optimize fixture and joint positions simultaneously. Matuszyk et al. [18] demonstrated the ability of an adaptable clamping sequence to control the overall dimensional variability in sheet metal assemblies. By using a FEM-based method, Gerbino et al. [19] conducted a parametric analysis for the optimal configuration of clamps to control gap between non-ideal parts. A novel robust algorithm for fixture design optimization was presented by Das et al. [20] to model variation within batches of non-ideal compliant assemblies. A robust assembly system design method, for selection of assembly line configuration, was described by Wang and Ceglarek [21]. Hu and Stecke [22] analyzed impact of assembly configurations on product quality variation and system performance. Mounaud et al. [23] studied the influence of assembly sequence on geometric deviations based on MIC. Xing et al. [24] introduced a novel ASP methodology through hybrid particle swarm optimization and genetic algorithm to generate and optimize assembly sequences. Based on the SVA-FEA methodology, Franciosa et al. [25] investigated different assembly configurations and fasten joints in the preliminary designing phase.

Table 1. Classification of literature review and the position of current work

Variation methods based on	Assembly process scheme	
	Single-station assembly system	*Multi-station assembly system*
Ideal part	Camelio et al. [16]; Liao and Wang [17]; Matuszyk et al. [18]	Wang and Ceglarek [6,21]; Mounaud et al. [23]; Xing and Wang [24]; Franciosa et al. [25]
Single non-ideal part (deterministic)	Hu and Stecke [22]; Gerbino et al. [19]	--
Batch of non-ideal parts (stochastic)	Das et al. [20]	**Proposed in this paper**

While much research is being carried out, variation propagation models and dimensional variation reduction approaches for MSA have yet to be fully deployed. The following research gaps are identified: (1) lack of models which consider non-ideal parts; current methods for MSA simulation assumed the parts are ideal while it has been proved that around 70% of all engineering changes are related to part fabrication errors; (2) lack of stochastic-driven simulations to model batches of non-ideal parts; traditional ASP-driven variation minimization approaches are not capable to take into consideration processes with batch assembly of non-ideal parts. Table 1 summarizes some of the methods developed over the years for variation reduction in design phase of single- and multi-station assembly systems.

To overcome the aforementioned limitations, this paper is to develop: (i) assembly sequence generation; (ii) variation propagation model and simulations for MSA considering batch of non-ideal parts, PCFR cycle, station-to-station repositioning error and spring-back phenomenon; (iii) *Assembly Configuration* (**AC**) index to provide a quantitative measurement of assembly sequence for given stochastic variation of parts being assembled; and (iv) stochastic robust optimization of assembly sequence and line configuration.

The paper is organized as follows: problem formulation is detailed in Section 2. Proposed methodology is established in Section 3. Industrial case study and conclusions are depicted in Sections 4 and 5, respectively.

2. Problem Formulation

Fig.1 shows a typical MSA system with K stations. Multiple operations at each station are modelled by PCFR cycle. Thus, at the i-th station ($\forall i = 1,...,N_{K-1}$), the PCFR$_i$ cycle is required to assemble the product in MSA.

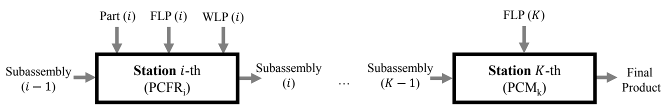

Fig. 1. Representation of K-station MSA with (K-1)-PCFR cycles

Parts/sub-assembly are first placed on fixture, and then clamped. Next, the parts are fastened by a joining technique. Finally, the sub-assembly is released from the fixtures. The sub-assembly is transferred to the downstream station. In the measurement station (K), the final product is firstly placed and clamped by checking fixture, and then variation of Key Product Characteristics (**KPCs**) are measured [2].

2.1. Definition of Assembly Configuration (AC) index in MSA

The key idea proposed in this paper is the concept of **AC** index, which allows to quantify the impact of assembly sequence for given variation associated to batch of non-ideal parts, which are assembled throughout the MSA system. The **AC** is presented by:

$$\mathbf{AC}=\{\mathrm{C},\mathrm{M}\} \tag{1}$$

where C describes the assembly sequence plan which includes the number of stations and sequence of assembled parts at each station. An assembly sequence set can be described by

$$\mathrm{C}=[(Station(1)),...,(Station(i)),...,(Measurement\ station(K))] \tag{2}$$

The assembly process data (M) comprise the Fixture Location Points (FLP(i)) and Welding Location Points (WLP(i)) at station i-th. For measurement station only FLP(K) is required as the checking fixture locations.

$$\mathrm{M}=[(\mathrm{FLP}(1),\mathrm{WLP}(1)),...,(\mathrm{FLP}(i),\mathrm{WLP}(i)),\ ...,\ (\mathrm{FLP}(K))] \quad (3)$$

2.2. Definition of KPC variations in MSA

Part deviations (non-ideal part) caused by stamping, handling or upstream assembly processes can be described by stochastic Key Control Characteristics (**KCCs**). Deviations patterns are assumed independent which means that the interactions between **KCCs** are not considered. In addition, stochastic distributions of each **KCC** are assumed Gaussian. The mathematical relationship between stochastic **KCCs** and part variations is expressed by:

$$\Delta \boldsymbol{P}_i^{t,j} = f_i^t\left(\mathbf{KCCs}^j\right) \quad (4)$$

where $\Delta \boldsymbol{P}_i^{t,j}$, and f_i^t are part variation and deviation generator function of t-th part at station i-th, for given j-th stochastic instance of **KCCs**. Stochastic instances can be generated by Monte-Carlo sampling or Polynomial Chaos [26]. This paper implemented Monte Carlo sampling approach.

The variation propagation mechanism in MSA is formally introduced by states space representation in Eqs. (5, 6).

$$\boldsymbol{X}^j(i) = \boldsymbol{X}^j(i-1) + \boldsymbol{U}^j(i) \quad \forall i = 1,..., K \quad (5)$$

$$\boldsymbol{U}^j(i) = F_i\left(\mathrm{FLP}(i), \mathrm{WLP}(i), \Delta \boldsymbol{P}_i^{t,j}\right) \quad (6)$$

where $\boldsymbol{X}^j(i)$ defines **KPCs** variation at station i-th, for given j-th stochastic instance of **KCCs.** F_i is the station "transfer function" which is associated to the PCFR_i cycle.

The **AC** index (ψ) is determined through a probabilistic approach and it is calculated as the integration of the **KPC** Probability Density Function (PDF) over the given allowance range (A_m), as formulated by

$$A_m = [LB_{\mathbf{KPC}_m}, UB_{\mathbf{KPC}_m}] \qquad \forall m = 1,..., \mathrm{N_{KPC}} \quad (7)$$

$$\psi = \int_{A_m} PDF_{\mathbf{KPC}_1 ... \mathbf{KPC}_m}(\boldsymbol{X}_{\mathbf{KPC}_1} ... \boldsymbol{X}_{\mathbf{KPC}_m})\, d\boldsymbol{X}_{\mathbf{KPC}_1} ... d\boldsymbol{X}_{\mathbf{KPC}_m} \quad (8)$$

where $\mathrm{N_{KPC}}$ is the number of **KPC**. The index value represents the compliance percentage of the **KPCs** variations with design requirements. Therefore, the optimum **AC** has the maximum index among the different **AC** indexes.

3. Proposed methodology

A MSA system can have various configurations and assembly sequences which can produce different product quality. To evaluate the produced product quality, it is essential to have an analytical tool with capability to model and simulate variation propagation in MSA system. In this section, an FEM-based approach is developed to examine product dimensional quality produced via a variety of assembly configurations (**AC**). As shown in Fig. 2, the proposed methodology consists of three main modules: (1) Assembly sequence generation, (2) Multi-station assembly simulation; and, (3) Stochastic robust optimization.

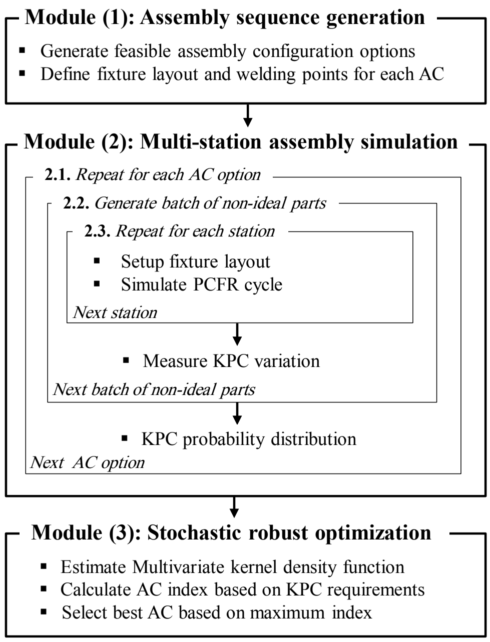

Fig. 2. Proposed methodology flowchart

3.1. Assembly sequence generation

ASP is a concept in which all feasible assembly configurations which includes assembly sequences are generated based on a liaison graph, assembly mode and sub-assembly patterns. In graph theory, an assembly set is described through a directed or undirected liaison graph $G = \{V, E\}$, where V is a set of parts and E is a set of connection lines (Fig. 3a). The precedence relations among an assembly are comprehended easily by an adjacency matrix (Fig. 3b). All serial sequences can be generated through Breadth-First Search (BFS) algorithm. Parallel sub-assemblies are created in two stages. Firstly, a part is selected as base part. Secondly, all parts connected with the part are probed. Finally, the sub-assemblies are generated from different combinations among the parts. All parallel sub-assemblies can be searched by repeating the BFS steps [27].

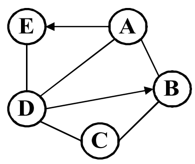

$$R = \begin{bmatrix} 0 & 1 & 0 & 1 & -1 \\ 1 & 0 & 1 & -1 & 0 \\ 0 & 1 & 0 & 1 & 0 \\ 1 & -1 & 1 & 0 & 1 \\ -1 & 0 & 0 & 1 & 0 \end{bmatrix}$$

(a) **(b)**

Fig. 3. (a) Directed liaison graph, (b) An adjacency matrix.

Three typical feasibility constraints are usually used to ensure that the generated assembly sequences are indeed feasible: (1) Geometric interference constraints, (2) Stability constraints, and (3) Part and tools accessibility constraints. They can be examined by the adjacency matrix and designer experience [28]. All assembly sequences are assessed by the constraints and the infeasible ones are omitted. For instance, the 4-station assembly configuration in Fig. 3 can be shown as

$$\mathrm{C}=[\underbrace{(\overbrace{\{A\}}^{\text{part}},\overbrace{\{B\}}^{\text{part}},\overbrace{\{C\}}^{\text{part}})}_{\text{station}_1},\underbrace{(\overbrace{\{A,B,C\}}^{\text{subassembly}},\overbrace{\{D\}}^{\text{part}})}_{\text{station}_2},\underbrace{(\overbrace{\{A,B,C,D\}}^{\text{subassembly}},\overbrace{\{E\}}^{\text{part}})}_{\text{station}_3},\underbrace{(\overbrace{\{A,B,C,D,E\}}^{\text{final product}})}_{\text{measurment station}}] \quad (9)$$

3.2. Multi-station assembly simulation

Dimensional variations simulations of the MSA system are carried out in module (2) (Fig. 2). In this study, Variation Response Methodology (VRM) is used for modelling single-PCFR cycle. VRM was implemented in MatLAB® environment, which allows defining and controlling features' specifications quickly such as locators (*N-2-1*), clamps, welding guns, and contact pairs. The FE simulations are executed using Cosmol Multiphusics® routines [29]. This methodology consists of four principal steps; in the first step, the FE model is derived from the nominal geometry through quadratic/triangle elements and non-ideal parts are created by the Morphing Mesh Producers (MMP). Part deviation is defined by a set of **KCC** parameters [13]. Fixture layout is determined as boundary conditions according to an *N-2-1* scheme. Finally, the frictionless contact pairs, part thickness, and elastic mechanical properties are defined subsequently. For simplicity, local thermal effects are neglected. As shown in Fig. 4, four consecutive FE runs are required for PCFR simulation. Three runs are related to the positioning, closing and releasing resistance-spot-welding (RSW) guns. The fourth simulation is relevant to clamps releasing (spring-back simulation) and setup new fixture layout for the sub-assembly at the next station. In this study, the placing and clamping phases are performed simultaneously, and the effect of welding sequence has not been considered.

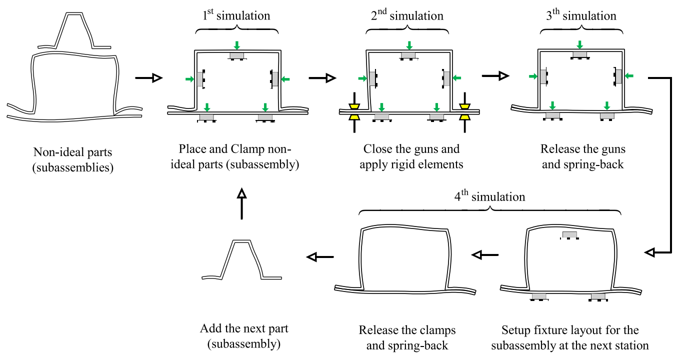

Fig. 4. Multi-station assembly process simulation

The **KPC** variation due to the FE simulations is derived by "transfer function". For *i*-th station, F_i is described by

$$F_i = \begin{cases} \boldsymbol{Q}_i^j(r) & \text{for sub-assembly}(i-1) \\ \Delta \boldsymbol{P}_i^{t,j} + \boldsymbol{Q}_i^j(r) & \text{for part}(i) \end{cases} \quad \forall r = 1 \text{ to } 4 \tag{10}$$

where $\boldsymbol{Q}_i^j(r)$ is displacement field coming from *r*-th FE run results. During the fastening phase, the welding points on the parts should be constrained to move together using multi-point constraints. Therefore, the rigid elements are defined in order to couple nodes. To simulate the elastic spring-back, the residual stresses are applied to any part of the assembly within two steps: (i) RSW guns releasing (σ_{fast}); (ii) clamps releasing (σ_{pos}). Thereafter, the sub-assembly is transferred to the downstream station and repositioned by other fixture layout, and then the part (sub-assembly) will be assembled to it. This process continues until the assembly set is completed. In this paper, the **KPC** variation is presented by the sum of deviations in the *X*-, *Y*- and *Z*-directions, as calculated by Eq. (11) at measurement station.

$$\boldsymbol{X}_{\mathbf{KPC}_m}^{j} = \sqrt{\left(\delta_{\mathbf{KPC}_m}^{j,X}\right)^2 + \left(\delta_{\mathbf{KPC}_m}^{j,Y}\right)^2 + \left(\delta_{\mathbf{KPC}_m}^{j,Z}\right)^2} \tag{11}$$

Since part and tool deviations are inherently stochastic, the **KPC** variations should be presented trough the probability distribution through the PDF.

3.3. Stochastic robust optimization

The **KPC** probability distributions obtained from stochastic simulations in Section 3.2 and the allowed ranges A_m are considered as inputs in module (3). Since the MSA is a non-linear and complex process, the PDF cannot be estimated through parametric model assuming normal distribution. On other hand, the number of **KPC** is usually more than one. Hence, multivariate Kernel Density Estimation (KDE) is used as a non-parametric PDF estimator [30]. Let $\boldsymbol{\lambda}_1,\ldots,\boldsymbol{\lambda}_j,\ldots,\boldsymbol{\lambda}_{N_{MC}}$ be a sample of m-variate **KPC** variation vectors drawn from a common distribution described by

$$PDF_{\mathbf{KPC}_1\ldots\mathbf{KPC}_m}(\boldsymbol{\lambda}) = \frac{1}{N_{MC}} \sum_{j=1}^{N_{MC}} K_{\mathbf{H}}(\boldsymbol{\lambda} - \boldsymbol{\lambda}_j) \tag{12}$$

where $\boldsymbol{\lambda} = (\boldsymbol{X}_1,\ldots,\boldsymbol{X}_m)$ and $\boldsymbol{\lambda}_j = (\boldsymbol{X}_{j1},\ldots,\boldsymbol{X}_{jm})$, m is the number of **KPCs**, $K_{\mathbf{H}}$ is the kernel smoothing function, N_{MC} is number of Monte-Carlo samples, and **H** is the bandwidth matrix. In this study, the smoothing function is assumed to be normal kernel which is described by

$$K_{\mathbf{H}}(\boldsymbol{\lambda}) = (2\pi)^{-\frac{m}{2}} |\mathbf{H}|^{-\frac{1}{2}} \exp\left(-\frac{\boldsymbol{\lambda}^T \mathbf{H}^{-1} \boldsymbol{\lambda}}{2}\right) \tag{13}$$

The bandwidth of the kernel is a free parameter which exhibits a strong effect on the resulting estimate. The optimal value for the bandwidth based on Silverman's rule of thumb is expressed by Eq. (14) that minimizes the mean integrated squared error [30].

$$\sqrt{\mathbf{H}_{mm}} = \sigma_m \left\{4/(m+2)n\right\}^{1/(m+4)} \tag{14}$$

where σ_m is the standard deviation of the m-th **KPC** and $\mathbf{H}_{ij} = 0,\, i \neq j$. As Fig. 5 shows, the **AC** index is determined through the integration of the kernel density functions over the given A_m , as formulated by

$$\psi = \int_{LB_{\mathbf{KPC}_1}}^{UB_{\mathbf{KPC}_1}} \cdots \int_{UB_{\mathbf{KPC}_m}}^{UB_{\mathbf{KPC}_m}} PDF_{\mathbf{KPC}_1\ldots\mathbf{KPC}_m}(\boldsymbol{X}_{\mathbf{KPC}_1} \ldots \boldsymbol{X}_{\mathbf{KPC}_m})\, d\boldsymbol{X}_1 \ldots d\boldsymbol{X}_m \tag{15}$$

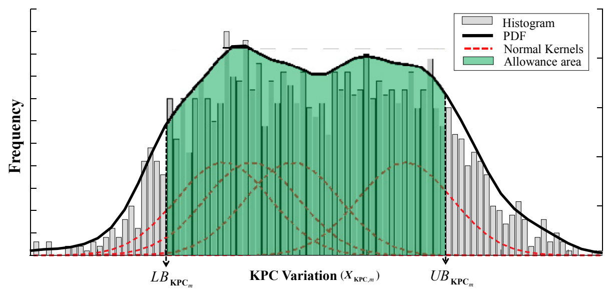

Fig. 5. **KPC** variation probability distribution obtained from KDE

4. Industrial case study and results

The proposed methodology was applied to an automotive front rail assembly (Fig. 6). The front rail consists of four parts which are welded by the RSW joining process.

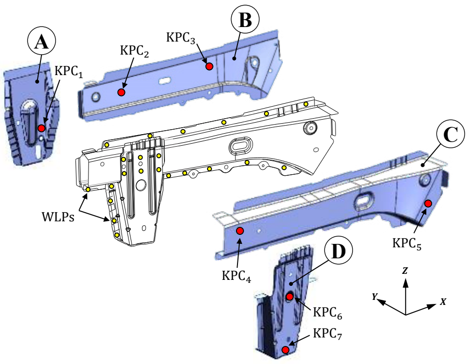

Fig. 6. The automotive front rail parts, KPCs, and WLPs

Nine feasible assembly sequence options in three categories (based on number of stations) are generated by assembly liaison graph (Fig. 7b), adjacency matrix (Fig. 7a) and the BFS algorithm, as listed in Table 2.

$$R=\begin{bmatrix}0 & -1 & 0 & 1\\ -1 & 0 & 1 & 0\\ 0 & 1 & 0 & -1\\ 1 & 0 & -1 & 0\end{bmatrix}$$

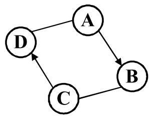

(a) **(b)**

Fig. 7. (a) The front rail adjacency matrix, (b) liaison graph

Table 2. The front rail assembly sequence options

Number of stations	Assembly sequence options
4	C_1=[({A},{B}),({A, B},{C}),({A,B,C},{D}),({A,B,C,D})]
	C_2=[({B},{C}),({B,C},{A}),({B,C, A},{D}),({B,C,A,D})]
	C_3=[({B},{C}),({B,C},{D}),({B,C,D},{A}),({B,C,D,A})]
	C_4=[({C},{D}),({C, D},{B}),({C,D,B},{A}),({C,D,B,A})]
	C_5=[({A},{B}) , ({C},{D}),({A, B},{C, D}),({A,B,C,D})]
3	C_6=[({A},{B},{C}),({A, B,C},{D}),({A,B,C,D})]
	C_7=[({B},{C},{D}),({B, C, D},{A}),({B,C,D,A})]
	C_8=[({B},{C}),({B, C},{A},{D}),{B,C,A,D})]
2	C_9=[({A},{B},{C},{D}),{A, B,C,D})]

The fixture layout of each station and WLPs are determined based on the both FLPs and Table 2. For instance, the assembly process data for C_1 is M_1, detailed in Table 3.

Table 3. Multi-station assembly process data (M_1)

i-th station	Assembly sequence	FLP(*i*) and WLP(*i*)
1st	{A}+{B}	FLP(1)={FLP_A,FLP_B}, WLP(1)={$WLP_{A,B}$}
2nd	{A,B}+{C}	FLP(2)={FLP_{AB},FLP_C}, WLP(2)={$WLP_{AB,C}$}
3th	{A,B,C}+{D}	FLP(3)={FLP_{ABC},FLP_D}, WLP(3)={$WLP_{ABC,D}$}
4th	{A,B,C,D}	FLP(4)={FLP_{ABCD}}

To simulate MSA process, the FE models are made of shell elements (Fig. 8a), and four contact pairs are defined at the part interfaces. MMP (f_i^t) is employed for non-ideal parts generation (Fig. 8b). Table 4 shows the **KCC** parameters and statistical values. The multi-PCFR simulation is iterated for each Monte-Carlo step (Fig. 2) and 500 iterations are used to generate part deviations.

Table 4. **KCC** parameters and statistical values assigned to the parts

Part	KCC (x, y, z)	R (mm)	Mean (mm)	Std Dev
A	(-550,520,330)	310	0	0.3
	(-525,520,130)		1	0.1
B	(-60,480,345)	840	0	0.3
	(-360,500,340)		1	0.1
	(-660,520,310)		0	0.2
C	(20,400,285)	850	0	0.3
	(-280,465,385)		1	0.1
	(-560,460,320)		0	0.2
D	(-540,465,120)	320	0	0.3
	(-460,460,285)		1	0.1

The fixture elements are applied to the parts and sub-assemblies as boundary constraints based on the FLPs (Fig. 8c). For any spot weld, 5 rigid links are used to couple the nodes. The final assembly is measured at the last station (Fig. 8d), and the **KPC** variations are calculated by Eq. (11).

The above procedure has been repeated to simulate nine assembly sequence options (C_1-C_9). The **KPC** probability density functions is obtained through multivariate KDE method (Fig. 9). The allowed range, A_m is set at [0, 2] mm for all the **KPC**. **AC** indexes are calculated by Eqs. (12-15) and shown in Table 5.

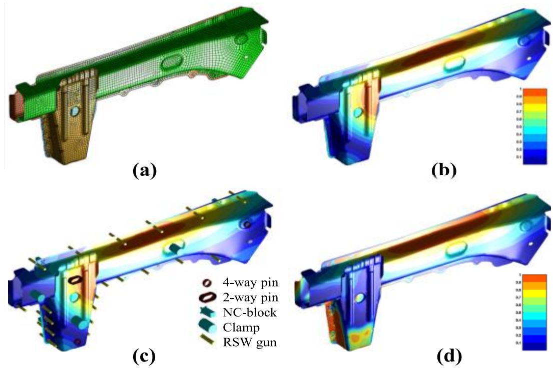

Fig. 8. (a) FEM mesh, (b) Non-ideal parts, (c) Setup locators and RSW gun, (d) Multi-PCFR simulation result

Table 5. The **AC** indexes for the automotive front rail assembly process

C_i	C_1	C_2	C_3	C_4	C_5	C_6	C_7	C_8	C_9
ψ	0.61	0.74	0.75	0.69	0.63	0.79	0.82	0.92	0.94

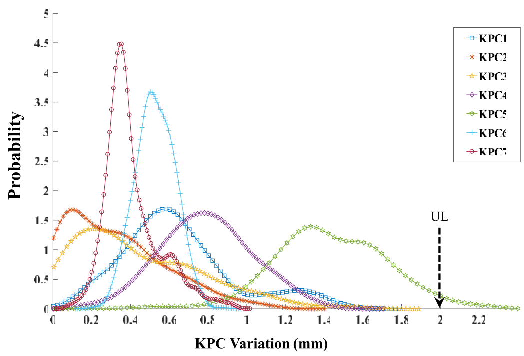

Fig. 9. The KPC probability distributions for the best **AC** ($\psi = 0.947$)

As the results imply, different **ACs** have strong impact on the dimensional quality of assembly systems. It can be seen in Table 5 that C_8 and C_9 are the best for controlling variations in the final assembly (the highest **AC** index), while C_1 and C_5 are the worst cases. Since part and tool deviations were considered, fixture layout and number of spot welds were constant during the assembly process. Thus, the part sequence and the number of stations are two major contributors to the variation of the final shape, meaning that if all assembly process was carried out at the single station (C_9), the dimensional problems would be affected by only the fixture and non-ideal part. Moreover, for each of extra stations added to the assembly line, an additional repositioning error source is introduced; therefore, the variation increases. On the other hand, in the assembly line with the same number of stations, it can be concluded that the **AC** index is dependent on the part (sub-assembly) stiffness. Hence, the assembly sequences from high- to low-part stiffness ($K_C > K_D > K_A > K_B$) have greater effect on the quality enhancement.

5. Conclusions

This study has presented a methodology for modeling MSA system considering batch of non-ideal parts and also development of **ACs** index for optimizing assembly sequence and number of stations. The important results are listed as follow:

- Modeling of station-to-station repositioning errors and spring-back phenomenon have been used for upgrading physics-driven assembly simulation in MSA, in which an analytical tool is developed for assessment and selection of the **AC** based on the quality criteria.
- It has been shown in the case study that the assembly process success rate (**AC** index) to meet the design requirements varied within in the wide range (61%- 94%). This means that the assembly sequence and number of stations affect dimensional errors intensively.
- It was shown, as the number of stations increases in C_1-C_5 and C_6-C_7, due to stuck-up of individual errors from the station-to-station repositioning, tool, and sub-assemblies, a large amount of variation (lower **AC** index) occur in the final product.
- In the assembly process with the same number of stations and part deviations, the **AC** index is dependent on the part (sub-assembly) stiffness and deviation. Therefore, it is recommended to select the assembly sequences according to the high- to low-part (sub-assembly) stiffness order.

Acknowledgements

The authors wish to thank School of Mechanical Engineering at University of Tehran (Iran) and Digital Lifecycle Management group at University of Warwick (UK) for their invaluable cooperation during this research. This study was partially supported by the UK EPSRC project EP/K019368/1: "Self-Resilient Reconfigurable Assembly Systems with In-process Quality Improvement."

References

[1] Shi J. Stream of variation modeling and analysis for multistage manufacturing processes, CRC press; 2006, p. 117–40.
[2] Ceglarek D, Shi J, Wu SM. A Knowledge-Based Diagnostic Approach for the Launch of the Auto-Body Assembly Process. J Eng Ind 1994;116:491-99.
[3] Camelio J, Hu SJ, Ceglarek D. Modeling variation propagation of multi-station assembly systems with compliant parts. J Mech Des 2003;125:673–81.
[4] Liu SC, Hu SJ. Variation simulation for deformable sheet metal assemblies using finite element methods. J Manuf Sci Eng 1997;119:368–74.
[5] Chang M, Gossard DC. Modeling the assembly of compliant, non-ideal parts. CAD Comput Aided Des 1997;29:701–8.
[6] Wang H, Ceglarek D. Variation propagation modeling and analysis at preliminary design phase of multi-station assembly systems. Assem Autom 2009;29:154–66.
[7] Hu SJ, Koren Y. Stream-of-Variation Theory for Automotive Body Assembly. CIRP Ann - Manuf Technol 1997;46:1–6.
[8] Jin J, Shi J. State Space Modeling of Sheet Metal Assembly for Dimensional Control. J Manuf Sci Eng 1999;121:756–62.
[9] Ding Y, Ceglarek D, Jianjun Shi. Modeling and diagnosis of multistage manufacturing processes: Part I state space model. Japan-USA Symp. Flex. Autom., At Ann Arbor, MI, USA: 2000.
[10] Xie K, Wells L, Camelio JA, Youn BD. Variation propagation analysis on compliant assemblies considering contact interaction. J Manuf Sci Eng 2007;129:934–42.
[11] Ungemach G, Mantwill F. Efficient Consideration of Contact in Compliant Assembly Variation Analysis. J Manuf Sci Eng 2008;131:11005.
[12] Gerbino S, Patalano S, Franciosa P. Statistical variation analysis of multi-station compliant assemblies based on sensitivity matrix. Int J Comput Appl Technol 2008;33:12–23.
[13] Franciosa P. Modeling and Simulation of Variational Rigid and Compliant Assembly for Tolerance Analysis. 2009.
[14] Franciosa P, Gerbino S, Patalano S. Variation analysis of compliant assemblies: a comparative study of a multi-station assembly. An Ing Graf 2010;21:45–52.
[15] Franciosa P, Gerbino S, Patalano S. Simulation of variational compliant assemblies with shape errors based on morphing mesh approach. Int J Adv Manuf Technol 2011;53:47–61.
[16] Camelio J, Hu SJ, Ceglarek D. Impact of Fixture Design on Sheet Metal Assembly Variation. J Manuf Syst 2004;23:182–93.
[17] Liao X, Wang GG. Simultaneous optimization of fixture and joint positions for non-rigid sheet metal assembly. Int J Adv Manuf Technol 2008;36:386–94.
[18] Matuszyk TI, Cardew-Hall M, Rolfe BF. The effect of clamping sequence on dimensional variability in sheet metal assembly. Virtual Phys Prototyp 2007;2:161–71.
[19] Gerbino S, Franciosa P, Patalano S. Parametric variational analysis of compliant sheet metal assemblies with shell elements. Procedia CIRP 2015;33:339–44.
[20] Das A, Franciosa P, Ceglarek D. Fixture Design Optimisation Considering Production Batch of Compliant Non-Ideal Sheet Metal Parts. Procedia Manuf 2015;1:157–68.
[21] Wang H, Ceglarek D. Quality-driven sequence planning and line configuration selection for compliant structure assemblies. CIRP Ann - Manuf Technol 2005;54:31–5.
[22] Hu SJ, Stecke KE. Analysis of automotive body assembly system configurations for quality and productivity. Int J Manuf Res 2009;4:281–305.
[23] Mounaud M, Thiébaut F, Bourdet P, Falgarone H, Chevassus N. Assembly sequence influence on geometric deviations propagation of compliant parts. Int J Prod Res 2011;49:1021–43.
[24] Xing Y, Wang Y. Assembly sequence planning based on a hybrid particle swarm optimisation and genetic algorithm. Int J Prod Res 2012;50:7303–12.
[25] Franciosa P, Gerbino S, Patalano S. A computer-aided tool to quickly analyse variabilities in flexible assemblies in different design scenarios. Int J Prod Dev 2013;18:112-33.
[26] Franciosa P, Gerbino S, Ceglarek D. Fixture Capability Optimisation for Early-stage Design of Assembly System with Compliant Parts Using Nested Polynomial Chaos Expansion. Procedia CIRP 2016;41:87–92.
[27] Xing Y, Chen G, Lai X, Jin S, Zhou J. Assembly sequence planning of automobile body components based on liaison graph. Assem Autom 2007;27:157–64.
[28] Wang L, Keshavarzmanesh S, Feng H-Y, Buchal RO. Assembly process planning and its future in collaborative manufacturing: a review. Int J Adv Manuf Technol 2009;41:132-44.
[29] Franciosa P, Das A, Yilmazer S, Gerbino S, Ceglarek D. Variation Response Method (VRM): a Kernel for Dimensional Management Simulation of non-ideal Compliant Parts. WMG DLM group; 2015.
[30] Silverman BW. Density estimation for statistics and data analysis. vol. 26. CRC press; 1986.